

Topological Bose-Mott insulators in one-dimensional non-Hermitian superlattices

Zhihao Xu^{1,2,3,4,*} and Shu Chen^{2,5,6,†}

¹*Institute of Theoretical Physics, Shanxi University, Taiyuan 030006, China*

²*Beijing National Laboratory for Condensed Matter Physics,*

Institute of Physics, Chinese Academy of Sciences, Beijing 100190, China

³*Collaborative Innovation Center of Extreme Optics, Shanxi University, Taiyuan 030006, P.R.China*

⁴*State Key Laboratory of Quantum Optics and Quantum Optics Devices,*

Institute of Opto-Electronics, Shanxi University, Taiyuan 030006, P.R.China

⁵*School of Physical Sciences, University of Chinese Academy of Sciences, Beijing, 100049, China*

⁶*Yangtze River Delta Physics Research Center, Liyang, Jiangsu 213300, China*

We study topological properties of Bose-Mott insulators in one-dimensional non-Hermitian superlattices, which may serve as effective Hamiltonians for cold atomic optical systems with either two-body loss or one-body loss. We find that in strongly repulsive limit, the Mott insulator states of the Bose-Hubbard model with a finite two-body loss under integer fillings are topological insulators characterized by a finite charge gap, nonzero integer Chern numbers and nontrivial edge modes in low-energy excitation spectrum under open boundary condition. The two-body loss suppressed by the strong repulsion results in a stable topological Bose-Mott insulator which behaves similar properties as the Hermitian case. However, for the non-Hermitian model related to the one-body loss, we find the non-Hermitian topological Mott insulators are unstable with a finite imaginary excitation gap.

PACS numbers:

Introduction. - Non-Hermitian topological systems have attracted much attention in the past years with the aid of the fast development of topological photonics [1–8]. Since the non-Hermitian systems possess more fundamental nonspatial symmetries, their topological classification goes beyond the standard ten classes of the corresponding Hermitian systems [9–16]. The non-Hermitian systems have been shown to exhibit many exotic properties without Hermitian counterparts [17–33], including half-integer topological invariants [24–29], non-Hermitian skin effect (NHSE) and breakdown of bulk-boundary correspondence in some non-reciprocal system [9, 30–50]. Recently, exploring topological phases in interacting non-Hermitian systems has also been addressed in several works [51, 52].

Due to their highly controllability, one-dimensional (1D) optical superlattices, which can be realized by superimposing two 1D optical lattices with commensurate wavelengths, have provided an ideal playground for exploring topologically nontrivial phases [53–64]. The interplay between many-body interaction and single-particle band topology can lead to intriguing correlated states exhibiting nontrivial topological properties, e.g., fractional topological states [57, 58] and topological Mott insulators (TMIs) [59–64] in the interacting superlattice systems. Recent experimental progress demonstrate that the optical lattice systems may be a controllable candidate for studying the quantum open systems by introducing a dissipation process [65], which can be effectively described by an effective non-Hermitian Hamiltonian under certain condition. So far, different kinds of literatures on the effect of the dissipation have been reported due to the particle loss or photon scattering [66–79]. Especially, the

two-body loss on quantum many-body systems is realized in the form of inelastic collisions which can be widely controlled [80–84]. One can tune the inelastic two-body scattering via a photo-association resonance in a bosonic or fermionic system, where a delay of the melting of the Mott insulating state was detected [83, 84].

Motivated by these progresses, in this work we study the realization of topological Mott phase in 1D non-Hermitian superlattice systems. For an interacting bosonic gas trapped in a superlattice with an integer band filling factor, a TMI is in the formation of the Mott phase characterized by a nontrivial topological invariant [59, 60]. When we consider a non-Hermitian system, its eigenenergies are generally complex and natural questions arise here are whether the Mott phase still exists and how to characterize the non-Hermitian TMI?

Model and method. - To address these problems, we first consider interacting bosons trapped in a 1D two-periodic optical lattice with the Hamiltonian described by $H_{\text{BH}} = H_0 + H_I$ with

$$H_0 = - \sum_j J(j, \theta) (\hat{b}_j^\dagger \hat{b}_{j+1} + H.c.) + \sum_j \frac{V(j, \theta)}{2} \hat{n}_j, \quad (1)$$

and

$$H_I = \frac{U}{2} \sum_j \hat{n}_j (\hat{n}_j - 1), \quad (2)$$

Here, \hat{b}_j is the annihilation operator of bosons at site j , $\hat{n}_j = \hat{b}_j^\dagger \hat{b}_j$ is the number operator of bosons, and the alternating hopping strengths are given by $J(j, \theta) = J[1 + \delta \sin(\pi j + \theta)]$ with the dimerization strength δ and

J being set as the energy unit ($J = 1$). The on-site potential is given by $V(j, \theta) = V \cos(\pi j + \theta)$ with $V \cos \theta$ denoting the energy offset between neighboring sites for real phase θ of the potential. The interaction strength $U = U_r$ is always real and can be experimentally controlled by the Feshbach resonance. Complex-valued interactions can emerge in some effective Hamiltonians of ultracold atomic systems induced by considering the inelastic processes between different orbitals which give rise to two-particle loss.

When atoms undergo inelastic collisions, the scattered atoms are lost from the system. The atom losses are described by a quantum master equation:

$$\begin{aligned} \partial_t \rho(t) = & -i[H, \rho(t)] - \frac{1}{2}\gamma \sum_j (L_j^\dagger L_j \rho(t) + \rho(t) L_j^\dagger L_j \\ & - 2L_j \rho(t) L_j^\dagger), \end{aligned} \quad (3)$$

where $\rho(t)$ is the density matrix of the atomic gas, L_j is a Lindblad operator at site j which describes a loss with the rate $\gamma > 0$. The process of two-particle loss can be described by setting $L_j \rightarrow \hat{b}_j \hat{b}_j$. Considering the short time evolution, the quantum-jump term can be negligible and the dynamical evolution is described by

$$\partial_t \rho(t) = -i(H_{\text{eff}}^{(1)} \rho(t) - \rho(t) H_{\text{eff}}^{(1)}), \quad (4)$$

where $H_{\text{eff}}^{(1)} = H_0 + H_I$ is an effective Hamiltonian with the interaction amplitude U taking a complex value

$$U = U_r - i\gamma. \quad (5)$$

Here $U_r \geq 0$ represents the repulsive interaction and $\gamma \geq 0$ the rate of loss.

When $U = 0$, the Hamiltonian reduces to the topologically nontrivial Rice-Mele model [85]. The energy spectrum in momentum space with momentum k is $\varepsilon_{\pm} = \pm\sqrt{2 + V^2 \cos^2 \theta/4 + 2\delta^2 \sin^2 \theta} + 2(1 - \delta^2 \sin^2 \theta) \cos k$ and the energy gap is $\Delta_b = 2\sqrt{V^2 \cos^2 \theta/4 + 4\delta^2 \sin^2 \theta}$. Fig. 1(a) shows the single-particle energy spectrum of Rice-Mele model as the function of θ with $\delta = 0.6$, $V = 2$ and $\theta = \pi/4$ under open boundary condition (OBC). As the phase shift θ varying from 0 to 2π , the edge states connecting two bulk spectra emerge in the gap regime which characterizes the topologically nontrivial feature.

When the repulsive interaction U_r is considered, the bosonic system with an integer band filling factor $\nu = N/N_{\text{cell}}$ can enter in a Mott phase, where N , L and $N_{\text{cell}} = L/2$ represent the number of bosons, lattice site and the unit cell of the system, respectively. We can calculate the charge gap defined as

$$\Delta_c = \frac{1}{2}[E_0(N+1) + E_0(N-1)] - E_0(N) \quad (6)$$

by numerically diagonalizing the Hamiltonian H_{BH} , where $E_0(N)$ represents the ground state energy of the

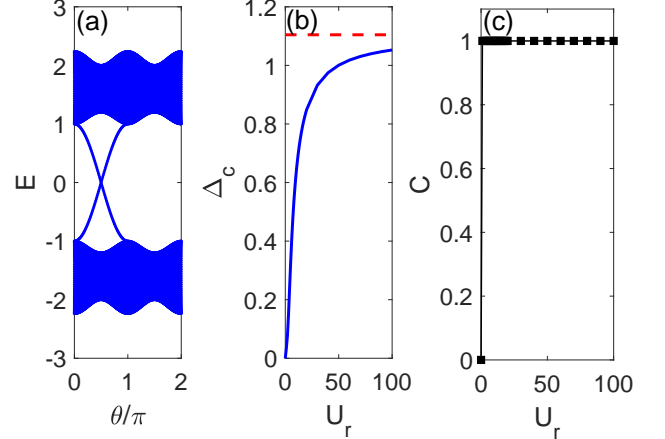


FIG. 1: (Color online) (a) Single-particle energy spectrum of Rice-Mele model as the function of θ under OBC. (b) The charge gap Δ_c as the function of U_r for the Hermitian case with $L = 14$ and $\nu = 1$ under PBC. The dashed line denotes $\Delta_b/2 = 1.1045$. (c) The Chern numbers versus U_r with $\nu = 1$. Here, $\delta = 0.6$ and $V = 2$.

N -boson system. Fig. 1(b) shows the charge gap Δ_c versus U_r for the Hermitian case H_{BH} with $L = 14$, $\delta = 0.6$, $V = 2$, $\theta = \pi/4$ and $\nu = 1$ under periodic boundary condition (PBC). In the small U_r limit, the charge gap $\Delta_c \rightarrow 0$ and the charge gap Δ_c grows with the increase of U_r . In the strongly repulsive limit, Δ_c tends to $\Delta_b/2$, as predicted by applying the Bose-Fermi mapping [59]. Our results indicate that a Mott-insulator phase emerges in the large U_r case.

The topological feature of the Mott-insulator state can be characterized by the many-body Chern number in the two-dimensional (2D) parameter space (φ, θ) [57, 59, 60]. Here, we introduce the twist boundary condition which is corresponding to a shift momentum $k = (2\pi m + \varphi)/N_{\text{cell}}$ in Brillouin zone with φ being a generalized boundary phase and $m = 0, 1, \dots, N_{\text{cell}} - 1$. The many-body Chern number for the Hermitian case is defined as $C = \frac{1}{2\pi} \int d\varphi d\theta B(\varphi, \theta)$ with the Berry curvature $B(\varphi, \theta) = \text{Im} \left(\langle \frac{\partial \psi}{\partial \theta} | \frac{\partial \psi}{\partial \varphi} \rangle - \langle \frac{\partial \psi}{\partial \varphi} | \frac{\partial \psi}{\partial \theta} \rangle \right)$. When the Mott insulator is formed for $\nu = 1$, the corresponding state has the Chern number $C = 1$, indicating that the Mott insulator is topologically nontrivial, i.e., the formation of TMI. As shown in Fig. 1(c), even for a small U_r , the topological number C already approaches to 1. Our numerical calculations demonstrate that the TMI emerges with the increase of U_r , which is consistent with previous studies [59, 60].

Non-Hermitian TMI. Now we study the non-Hermitian effect induced by the imaginary part of U . As a concrete example, we consider the system described by Hamiltonian $H_{\text{eff}}^{(1)}$ with $\nu = 1$, $\delta = 0.6$, $V = 2$,

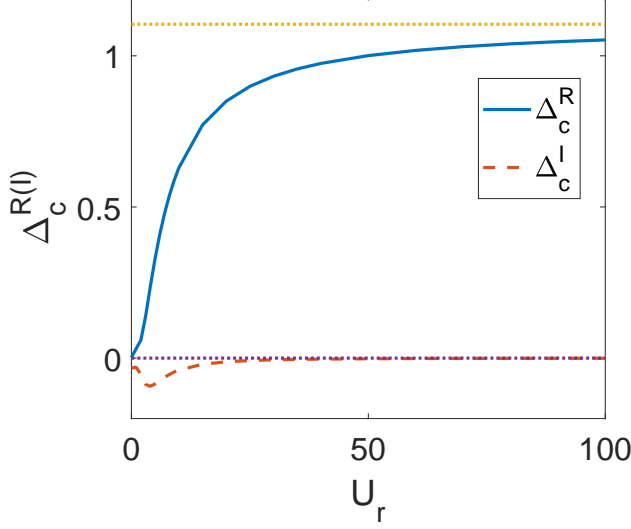


FIG. 2: (Color online) The real part Δ_c^R and the imaginary part Δ_c^I of the charge gap as the function of U_r for the Hamiltonian $H_{\text{eff}}^{(1)}$ with $L = 14$, $\nu = 1$, $\delta = 0.6$, $V = 2$, $\theta = \pi/4$ and $\gamma = 1$ under PBC. The orange dotted line denotes $\Delta_b/2 = 1.1045$ and the value of the purple dotted line is zero.

$\theta = \pi/4$ and $\gamma = 1$, and calculate the charge gap Δ_c defined by Eq. (6). Here, due to the complex energy spectrum for a non-Hermitian system, we define $E_0(N)$ as the the ground state energy for the N -boson system with the minimum value of the real-part. Correspondingly, the real part of the charge gap for non-Hermitian case, is defined as $\Delta_c^R = \text{Re}(\Delta_c)$ and the imaginary part of the charge gap $\Delta_c^I = \text{Im}(\Delta_c)$ is also calculated. Fig. 2 shows Δ_c^R and Δ_c^I as the function of U_r under PBC. For $U_r = 0$, the real part of the charge gap $\Delta_c^R \rightarrow 0$ and Δ_c^I takes a finite value. The real part of the charge gap Δ_c^R shows a monotonic increase with the increasing of U_r and tends to $\Delta_b/2$ in the strongly repulsive limit. However, with the increase of U_r , the absolute value of Δ_c^I firstly increases and then decreases when $U_r > 3.76$. In the large U_r limit, $\Delta_c^I \rightarrow 0$ and two-body collisions are strongly suppressed which leads to the decreasing of the atomic loss, indicating that a stable Mott insulator emerges in the strongly interacting limit.

To characterize the topological feature, we now construct the many-body Chern number for the non-Hermitian case. In 2D parameter space of (φ, θ) , the Chern number of the ground state for a non-Hermitian system is an integral invariant, which can be defined as

$$C^{\alpha\beta} = \frac{1}{2\pi} \int d\varphi d\theta B^{\alpha\beta}(\varphi, \theta), \quad (7)$$

where the Berry curvatures $B^{\alpha\beta}(\varphi, \theta) =$

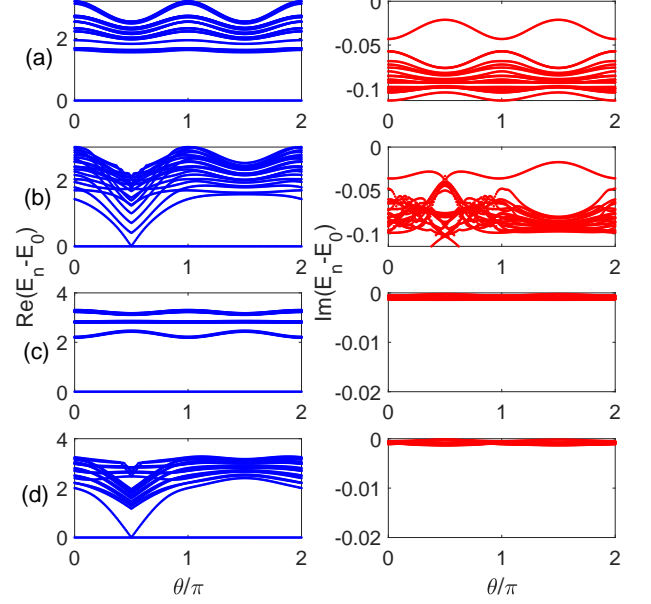


FIG. 3: (Color online) The real part (left column) and the imaginary part (right column) of the low-energy spectrum $E_n - E_0$ versus θ with different U_r , $L = 12$, $\nu = 1$, $\delta = 0.6$, $V = 2$ and $\gamma = 1$. (a) $U_r = 10$ under PBC; (b) $U_r = 10$ under OBC; (c) $U_r = 100$ under PBC; (d) $U_r = 100$ under OBC.

$\text{Im} \left(\langle \frac{\partial \psi^\alpha}{\partial \theta} | \frac{\partial \psi^\beta}{\partial \varphi} \rangle - \langle \frac{\partial \psi^\alpha}{\partial \varphi} | \frac{\partial \psi^\beta}{\partial \theta} \rangle \right)$ with $\alpha, \beta = R/L$. These definitions are a direct generalization of non-Hermitian Chern numbers [26] to the many-body systems. Here, the right eigenstates $|\psi^R\rangle$ and the left eigenstates $|\psi^L\rangle$ can be respectively defined as $H|\psi^R\rangle = E|\psi^R\rangle$ and $H^\dagger|\psi^L\rangle = E^*|\psi^L\rangle$ with the normalization condition $\langle \psi^\alpha | \psi^\beta \rangle = 1$. We numerically calculate four different Chern numbers C^{LL} , C^{LR} , C^{RL} and C^{RR} of the Hamiltonian $H_{\text{eff}}^{(1)}$ with $\nu = 1$, $\gamma = 1$ and different U_r . We find $C^{LL} = C^{LR} = C^{RL} = C^{RR} = 1$ for this non-Hermitian interacting boson system with finite repulsive U_r . In the large U_r limit, the stable Mott insulators are formed for $\nu = 1$, corresponding to the states with nontrivial Chern numbers, which show similar features as the Hermitian case and the stable Mott insulators are topologically nontrivial.

According to the bulk-edge correspondence, one may expect that the non-Hermitian TMIs also exhibit non-trivial edge states under OBC. In Fig. 3, we show the real part (left column) and the imaginary part (right column) of the low-energy spectrum $E_n - E_0$ versus θ with $\nu = 1$, $\gamma = 1$, $L = 12$, and various U_r under both PBC and OBC, where n marks the energy states to fulfill $\text{Re}(E_1) \leq \text{Re}(E_2) \leq \dots$. As shown in Figs. 3(a) and 3(c), there is an obvious gap of the real part of the low-energy spectrum between the ground state and the first

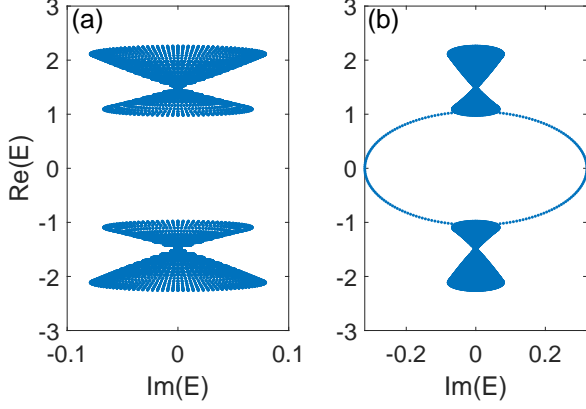


FIG. 4: (Color online) Complex energy spectrum of H_0^{NH} by rolling $\theta \in [0, 2\pi]$ with $\beta = 0.1\pi$, $\delta = 0.6$ and $V = 2$ under (a) PBC and (b) OBC.

excited state for systems with $U_r = 10$ and $U_r = 100$ under PBC, respectively. Correspondingly, the edge states emerge in the real gap regimes of the low-energy excitation spectrum under OBC. As the phase shift θ varies from 0 to 2π , the edge states connect the ground state to the excited band, as shown in Figs. 3(b) and 3(d) for systems with $U_r = 10$ and $U_r = 100$ under OBC, respectively. The real part of low-energy excitation spectrum for system with $U_r = 100$ of $H_{\text{eff}}^{(1)}$ exhibits almost the same behaviors as its corresponding Hermitian case. The imaginary part of low-energy excitation spectrum gradually converges to zero with the growth of U_r , indicating that the effect of the finite two-body loss is almost completely suppressed and a stable TMI exists in strongly repulsive limit.

TMI in the non-Hermitian Rice-Mele model.— Next we also consider another non-Hermitian extension of the Hamiltonian by taking a complex phase θ , i.e., $H_{\text{eff}}^{(2)} = H_0^{\text{NH}} + H_I$, where H_0^{NH} is obtained by replacing $\theta \rightarrow \theta + i\beta$ in H_0 with β being an imaginary phase shift. The non-Hermitian Hamiltonian H_0^{NH} may serve as an effective Hamiltonian related to some one-body loss processes [86, 87], and similar models have been studied in Ref. [88–90]. We take $\beta = 0.1\pi$ as an example for exhibiting our calculation results. In the absence of U_r , the energy gap in the complex-energy plane as defined in Ref. [26] is emergent for rolling $\theta \in [0, 2\pi]$ which is shown in Fig. 4(a) with $\delta = 0.6$ and $V = 2$ under PBC. When OBC is considered, the edge states emerge between the two bulk bands [see Fig. 4(b)], with the corresponding bulk state characterized by a nonzero band Chern number [26].

In the presence of the interaction, we first calculate the charge gap Δ_c versus U_r with $\beta = 0.1\pi$, $\delta = 0.6$, $V = 2$, $\theta = \pi/4$ and $L = 14$ under PBC, as shown in Fig. 5(a). With the increase of repulsion, both the real and imaginary parts of the charge gap Δ_c^R increase and

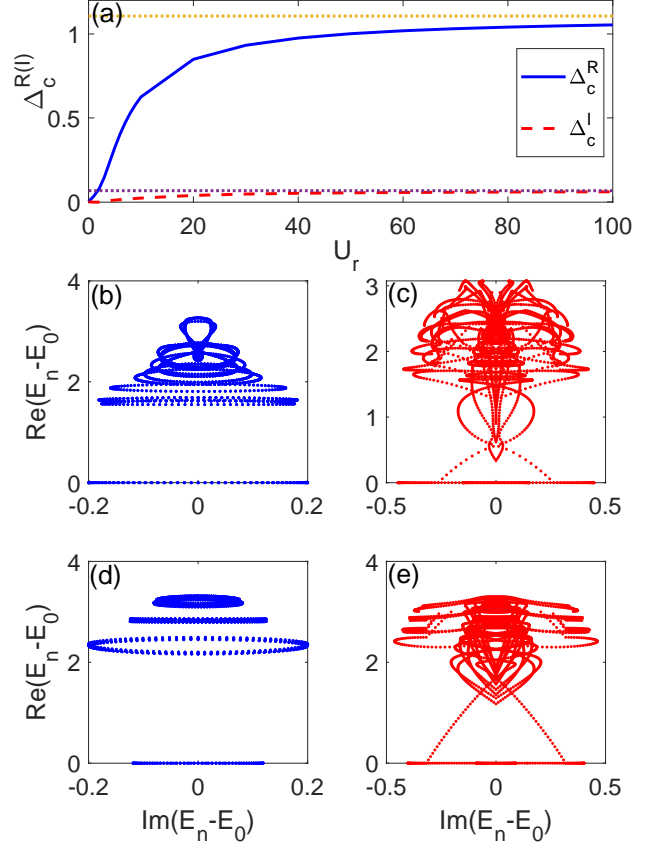


FIG. 5: (Color online) (a) The real part Δ_c^R and the imaginary part Δ_c^I of the charge gap as the function of U_r for the Hamiltonian $H_{\text{eff}}^{(2)}$ with $\theta = \pi/4$ under PBC. The value of the orange dotted line is equal to $\text{Re}(\Delta_b)/2 = 1.1065$ and the value of the purple dotted line amounts to $\text{Im}(\Delta_b)/2 = 0.0667$. (b)-(e) Low-energy excitation spectra of $H_{\text{eff}}^{(2)}$ by rolling $\theta \in [0, 2\pi]$. (b) $U_r = 10$ under PBC; (c) $U_r = 10$ under OBC; (d) $U_r = 100$ under PBC and (e) $U_r = 100$ under OBC. Here, $L = 14$, $\nu = 1$, $\delta = 0.6$, $V = 2$ and $\beta = 0.1\pi$.

in the strong repulsion, $\Delta_c^R \rightarrow \text{Re}(\Delta_b)/2 = 1.1065$ and $\Delta_c^I \rightarrow \text{Im}(\Delta_b)/2 = 0.0667$. A finite imaginary-valued gap indicates that the Mott phase will collapse in the long-time evolution. To characterize the topological property of the unstable Mott insulators, we numerically calculate the Chern number Eq. (7) defined in non-Hermitian case. When $U_r > 0$, the four Chern numbers are equal and $C^{LL} = C^{LR} = C^{RL} = C^{RR} = 1$. The existence of the nonzero Chern number implies the repulsively interacting system with an integer filling factor having nontrivial topological properties. The topological phase would exhibit nontrivial edge modes in the gap regions under OBC. We calculate the low-energy excitation spectra of $H_{\text{eff}}^{(2)}$ with $L = 14$, $\nu = 1$, $\delta = 0.6$, $V = 2$ and $\beta = 0.1\pi$

by rolling $\theta \in [0, 2\pi]$ shown in Figs. 5(b)-(e). As shown in Figs. 5(b) and 5(d), an obvious energy gap is shown between the ground state and the low-energy excitation states for $U_r = 10$ and 100 under PBC, respectively. Under OBC, as the phase shift θ varies from 0 to 2π , the low-energy spectra with $U_r = 10$ and 100 are shown in Figs. 5(c) and 5(e), respectively. The edge states connecting the ground states and low-energy part emerge in the gap and the position of the edge states continuously varies with the rolling of θ in the complex-energy plane. Specifically, the energies of the ground states and the edge modes exhibit a finite imaginary part which implies that the non-Hermitian TMIs with the one-body loss are formed, but due to the finite imaginary parts of the ground energies, the TMIs are unstable and shall be broken down during the time evolution.

Conclusions.- In summary, we have discussed topological Bose-Mott insulators in 1D non-Hermitian superlattices which are characterized by a finite charge gap, nonzero integer Chern numbers defined in non-Hermitian case and nontrivial edge modes in low-energy excitation spectrum under OBC. We found that for the non-Hermitian effect induced by a finite two-body loss, the nontrivial TMIs are stable in strong repulsion limit. However, for a non-Hermitian TMI associated with one-body loss, the low-energy excitation spectrum with a finite imaginary part suggests the TMI is unstable and shall collapse with time.

Note added: While main results of this manuscript were completed, we became aware of the similar works of [91, 92], which discuss the non-Hermitian topological Mott insulators in the interacting non-Hermitian Aubry-André-Harper models with different focus issues.

Z. Xu is supported by the NSFC (Grant No. 11604188) and STIP of Higher Education Institutions in Shanxi under Grant No. 2019L0097. S. Chen was supported by the NSFC (Grant No. 11974413) and the NKRPD of China (Grants No. 2016YFA0300600 and No. 2016YFA0302104). This work is also supported by NSF for Shanxi Province Grant No.1331KSC.

* Electronic address: xuzhihao@sxu.edu.cn

† Electronic address: schen@iphy.ac.cn

- [1] L. Lu, J. D. Joannopoulos, and M. Soljacic, Topological photonics, *Nat Photon*, **8**, 821 (2014).
- [2] T. Ozawa, H. M. Price, A. Amo, N. Goldman, M. Hafezi, L. Lu, M. Rechtsman, D. Schuster, J. Simon, O. Zilberberg, and I. Carusotto, Topological photonics, *Rev. Mod. Phys.* **91**, 015006 (2019).
- [3] A. Guo, G. J. Salamo, D. Duchesne, R. Morandotti, M. Volatier-Ravat, V. Aimez, G. A. Siviloglou, and D. N. Christodoulides, Observation of PT -symmetry breaking in complex optical potentials, *Phys. Rev. Lett.* **103**, 093902 (2009).
- [4] K. Ding, G. Ma, M. Xiao, Z. Q. Zhang, and C. T. Chan.

- Emergence, coalescence, and topological properties of multiple exceptional points and their experimental realization, *Phys. Rev. X*, **6**, 021007 (2016).
- [5] H. Xu, D. Mason, Luyao Jiang, and J. G. E. Harris, Topological energy transfer in an optomechanical system with exceptional points, *Nature*, **537**, 80 (2016).
- [6] B. Midya, H. Zhao, and L. Feng, Nonhermitian photonics promises exceptional topology of light, *Nat. Commun.* **9**, 2674 (2018).
- [7] V. M. Martinez Alvarez, J. E. Barrios Vargas, M. Berdakin, and L. E. F. Foa Torres, Topological states of non-Hermitian systems, *Eur. Phys. J. Spec. Top.* **227**, 1295 (2018).
- [8] A. Ghatak and T. Das, New topological invariants in non-Hermitian systems, *J. Phys.: Condens. Matter* **31**, 263001 (2019).
- [9] Z. Gong, Y. Ashida, K. Kawabata, K. Takasan, S. Higashikawa, and M. Ueda, Topological Phases of Non-Hermitian Systems, *Phys. Rev. X* **8**, 031079 (2018).
- [10] C. Liu, H. Jiang, and S. Chen, Topological classification of non-Hermitian systems with reflection symmetry, *Phys. Rev. B* **99**, 125103 (2019).
- [11] K. Kawabata, K. Shiozaki, M. Ueda, and M. Sato, Symmetry and topology in non-Hermitian physics, *Phys. Rev. X* **9**, 041015 (2019).
- [12] H. Zhou and J. Y. Lee, Periodic table for topological bands with non-Hermitian symmetries, *Phys. Rev. B* **99**, 235112 (2019).
- [13] C. Liu, and S. Chen, Topological classification of defects in non-Hermitian systems, *Phys. Rev. B* **100**, 144106(2019).
- [14] S. Lieu, Topological symmetry classes for non-Hermitian models and connections to the Bosonic BogoliubovCde Gennes equation, *Phys. Rev. B* **98**, 115135 (2018).
- [15] K. Kawabata, S. Higashikawa, Z. Gong, Y. Ashida, and M. Ueda, Topological unification of time-reversal and particle-hole symmetries in non-Hermitian physics, *Nat. Commun.* **10**, 297 (2019).
- [16] H. C. Wu, L. Jin, and Z. Song, Inversion symmetric non-Hermitian Chern insulator, *Phys. Rev. B* **100** 155117 (2019).
- [17] Y. Xu, S.-T. Wang, and L.-M. Duan, Weyl exceptional rings in a three-dimensional dissipative cold atomic gas, *Phys. Rev. Lett.* **118**, 045701 (2017).
- [18] N. Hatano and D. R. Nelson, Localization transitions in non-Hermitian quantum mechanics, *Phys. Rev. Lett.* **77**, 570 (1996).
- [19] M. S. Rudner and L. S. Levitov, Topological transition in a non-Hermitian quantum walk, *Phys. Rev. Lett.* **102**, 065703 (2009).
- [20] K. Esaki, M. Sato, K. Hasebe, and M. Kohmoto, Edge states and topological phases in non-Hermitian systems, *Phys. Rev. B* **84**, 205128 (2011).
- [21] B. Zhu, R. Lü, and S. Chen, PT symmetry in the non-Hermitian Su-Schrieffer-Heeger model with complex boundary potentials, *Phys. Rev. A* **89**, 062102 (2014).
- [22] Z. H. Xu, R. Zhang, S. Chen, L. B. Fu, and Y. B. Zhang, Fate of zero modes in a finite Su-Schrieffer-Heeger model with PT symmetry, *Phys. Rev. A* **101**, 013635 (2020).
- [23] C. Yu, Topological phase in a non-Hermitian PT symmetric system, *Phys. Lett. A* **379**, 1213 (2015).
- [24] T. E. Lee, Anomalous edge state in a non-Hermitian lattice, *Phys. Rev. Lett.* **116**, 133903 (2016).
- [25] D. Leykam, K. Y. Bliokh, C. Huang, Y. D. Chong, and F.

- Nori, Edge modes, degeneracies, and topological numbers in non-Hermitian systems, *Phys. Rev. Lett.* **118**, 040401 (2017).
- [26] H. Shen, B. Zhen, and L. Fu, Topological band theory for non-Hermitian Hamiltonians, *Phys. Rev. Lett.* **120**, 146402 (2018).
- [27] C. Yin, H. Jiang, L. Li, R. Lü and S. Chen, Geometrical meaning of winding number and its characterization of topological phases in one-dimensional chiral non-Hermitian systems, *Phys. Rev. A* **97**, 052115 (2018).
- [28] S. Lieu, Topological phases in the non-Hermitian Su-Schrieffer-Heeger model, *Phys. Rev. B* **97**, 045106 (2018).
- [29] H. Jiang, C. Yang, and S. Chen, Topological invariants and phase diagrams for one-dimensional two-band non-Hermitian systems without chiral symmetry, *Phys. Rev. A* **98**, 052116 (2018).
- [30] S. Yao and Z. Wang, Edge states and topological invariants of non-Hermitian systems, *Phys. Rev. Lett.* **121**, 086803 (2018).
- [31] V. M. Martinez Alvarez, J. E. Barrios Vargas, and L. E. F. Foa Torres, Non-Hermitian robust edge states in one dimension: anomalous localization and eigenspace condensation at exceptional points, *Phys. Rev. B* **97**, 121401(R) (2018).
- [32] Y. Xiong, Why does bulk boundary correspondence fail in some non-Hermitian topological models, *J. Phys. Commun.* **2**, 035043 (2018).
- [33] F. K. Kunst, E. Edvardsson, J. C. Budich, and E. J. Bergholtz, Biorthogonal bulk-boundary correspondence in non-Hermitian systems, *Phys. Rev. Lett.* **121**, 026808 (2018).
- [34] S. Yao, F. Song, and Z. Wang, Non-Hermitian chern bands, *Phys. Rev. Lett.* **121**, 136802 (2018).
- [35] L. Jin and Z. Song, Bulk-boundary correspondence in non-Hermitian systems, *Phys. Rev. B* **99**, 081103(R) (2019).
- [36] C. H. Lee and R. Thomale, Anatomy of skin modes and topology in non-Hermitian systems, *Phys. Rev. B* **99**, 201103(R) (2019).
- [37] K. Kawabata, K. Shiozaki, and M. Ueda, Anomalous helical edge states in a non-Hermitian chern insulator, *Phys. Rev. B*, **98**, 165148, (2018).
- [38] C. H. Lee, L. Li, and J. Gong, Hybrid higher-order skin-topological modes in non-reciprocal systems, *Phys. Rev. Lett.* **123**, 016805 (2019).
- [39] L. Herviou, J. H. Bardarson, and N. Regnault, Defining a bulk-edge correspondence for non-Hermitian Hamiltonians via singular-value decomposition, *Phys. Rev. A* **99**, 052118 (2019).
- [40] W. B. Rui, Y. X. Zhao, Andreas P. Schnyder, Classification of massive Dirac models with generic non-Hermitian perturbations, *Phys. Rev. B* **99**, 241110(R) (2019).
- [41] F. Song, S. Yao, and Z. Wang, Non-Hermitian Topological invariants in real space, *Phys. Rev. Lett.* **123**, 246801 (2019).
- [42] S. Longhi, Probing non-Hermitian skin effect and non-Bloch phase transitions, *Phys. Rev. Research* **1**, 023013 (2019).
- [43] H. Jiang, R. Lü, and S. Chen, Topological invariants, zero mode edge states and finite size effect for a generalized non-reciprocal Su-Schrieffer-Heeger model, arXiv:1906.04700 (2019).
- [44] Z. Ozcakmakli Turker and C. Yuce, Open and closed boundaries in non-Hermitian topological systems, *Phys. Rev. A* **99**, 022127 (2019).
- [45] L. Xiao, T. Deng, K. Wang, G. Zhu, Z. Wang, W. Yi, and P. Xue, Observation of non-Hermitian bulk-boundary correspondence in quantum dynamics, arXiv:1907.12566 (2019).
- [46] X. R. Wang, C. X. Guo, and S. P. Kou, Defective edge states and anomalous bulk-boundary correspondence in non-Hermitian topological systems, arXiv:1912.04024 (2019).
- [47] K. Yokomizo and S. Murakami, Non-Bloch band theory of non-Hermitian systems, *Phys. Rev. Lett.* **123**, 066404 (2019).
- [48] K. Zhang, Z. Yang, C. Fang, Correspondence between winding numbers and skin modes in non-hermitian systems, arXiv:1910.01131 (2019).
- [49] Z. Yang, K. Zhang, C. Fang, and J. Hu, Auxiliary generalized Brillouin zone method in non-Hermitian band theory, arXiv:1912.05499 (2019).
- [50] N. Okuma, K. Kawabata, K. Shiozaki, and M. Sato, Topological origin of non-Hermitian skin effects, arXiv:1910.02878 (2019).
- [51] W. Xi, Z. H. Zhang, Z. C. Gu, and W. Q. Chen, Classification of topological phases in one dimensional interacting non-Hermitian systems and emergent unitarity, arXiv:1911.01590 (2019).
- [52] T. Yoshida, K. Kudo, and Y. Hatsugai, Non-Hermitian fractional quantum Hall states, *Sci. Rep.* **9**, 16895 (2019).
- [53] L.-J. Lang, X. Cai, and S. Chen, Edge states and topological phases in one-dimensional optical superlattices, *Phys. Rev. Lett.* **108**, 220401 (2012).
- [54] Y. E. Kraus, Y. Lahini, Z. Ringel, M. Verbin, and O. Zeitler, Topological states and adiabatic pumping in quasicrystals, *Phys. Rev. Lett.* **109**, 106402 (2012).
- [55] S. Ganesan, K. Sun, and S. Das Sarma, Topological Zero-Energy Modes in Gapless Commensurate Aubry-Andre-Harper Models, *Phys. Rev. Lett.* **110**, 180403 (2013).
- [56] H. M. Guo and S. Chen, Kaleidoscope of symmetry-protected topological phases in one-dimensional periodically modulated lattices, *Phys. Rev. B* **91**, 041402 (2015).
- [57] Z. H. Xu, L. H. Li, and S. Chen, Fractional Topological states of dipolar fermions in one-dimensional optical superlattices, *Phys. Rev. Lett.* **110**, 215301 (2013).
- [58] T. S. Zeng, W. Zhu, D. N. Sheng, Fractional charge pumping of interacting bosons in one-dimensional superlattice, *Phys. Rev. B* **94**, 235139 (2016).
- [59] Z. H. Xu and S. Chen, Topological Mott insulators of ultracold atomic mixtures induced by interactions in one-dimensional optical superlattices, *Phys. Rev. B* **88**, 045110 (2013).
- [60] S.-L. Zhu, Z.-D. Wang, Y.-H. Chan, and L.-M. Duan, Topological Bose-Mott insulators in a one-dimensional optical superlattice, *Phys. Rev. Lett.* **110**, 075303 (2013).
- [61] F. Grusdt, M. Hönig, and M. Fleischhauer, Topological edge states in the one-dimensional superlattice Bose-Hubbard model, *Phys. Rev. Lett.* **110**, 260405 (2013).
- [62] T. Yoshida, R. Peters, S. Fujimoto, and N. Kawakami, Characterization of a Topological Mott Insulator in One Dimension, *Phys. Rev. Lett.* **112**, 196404 (2014).
- [63] Y. Kuno, K. Shimizu, and I. Ichinose, Various topological Mott insulators and topological bulk charge pumping in strongly- interacting boson system in one-dimensional superlattice, *New J. Phys.* **19**, 123025 (2017).
- [64] H. Hu, S. Chen, T.-S. Zeng, and C. Zhang, Topolog-

- ical Mott insulator with bosonic edge modes in one-dimensional fermionic superlattices, *Phys. Rev. A* **100**, 023616 (2019).
- [65] J. Li, A. K. Harter, J. Liu, L. de Melo, Y. N. Joglekar, and L. Luo, Observation of parity-time symmetry breaking transitions in a dissipative Floquet system of ultracold atoms, *Nat. Commun.* **10**, 855 (2019).
- [66] D. Witthaut, F. Trimborn, S. Wimberger, Dissipation induced coherence of a two-mode Bose-Einstein condensate, *Phys. Rev. Lett.* **101**, 200402 (2008).
- [67] F. Verstraete, M. M. Wolf, J. I. Cirac, Quantum computation and quantum-state engineering driven by dissipation, *Nat. Phys.* **5**, 633 (2009).
- [68] Y.-J. Han, Y.-H. Chan, W. Yi, A. J. Daley, S. Diehl, P. Zoller, L.-M. Duan, Stabilization of the p-wave superfluid state in an optical lattice, *Phys. Rev. Lett.* **103**, 070404 (2009).
- [69] E. G. Dalla Torre, E. Demler, T. Giamarchi, E. Altman, Quantum critical states and phase transitions in the presence of non-equilibrium noise, *Nat. Phys.* **6**, 806 (2010).
- [70] S. Diehl, A. Micheli, A. Kantian, B. Kraus, H. P. Büchler, P. Zoller, Quantum states and phases in driven open quantum systems with cold atoms, *Nat. Phys.* **4**, 878 (2008).
- [71] S. Diehl, A. Tomadin, A. Micheli, R. Fazio, P. Zoller, Dynamical phase transitions and instabilities in open atomic many-body systems, *Phys. Rev. Lett.* **105**, 015702 (2010).
- [72] A. Tomadin, S. Diehl, P. Zoller, Nonequilibrium phase diagram of a driven and dissipative many-body system, *Phys. Rev. A* **83**, 013611 (2011).
- [73] A. Le Boité, G. Orso, C. Ciuti, Steady-state phases and tunneling-induced instabilities in the driven dissipative Bose-Hubbard model, *Phys. Rev. Lett.* **110**, 233601 (2013).
- [74] I. Vidanović, D. Cocks, W. Hofstetter, Dissipation through localized loss in bosonic systems with long-range interactions, *Phys. Rev. A* **89**, 053614 (2014).
- [75] K. Stannigel, P. Hauke, D. Marcos, M. Hafezi, S. Diehl, M. Dalmonte, P. Zoller, Constrained dynamics via the Zeno effect in quantum simulation: Implementing non-Abelian lattice gauge theories with cold atoms, *Phys. Rev. Lett.* **112**, 120406 (2014).
- [76] Y. Ashida, S. Furukawa, M. Ueda, Quantum critical behavior influenced by measurement backaction in ultracold gases, *Phys. Rev. A* **94**, 053615 (2016).
- [77] H. P. Lüschen, P. Bordia, S. S. Hodgman, M. Schreiber, S. Sarkar, A. J. Daley, M. H. Fischer, E. Altman, I. Bloch, and U. Schneider, Signatures of Many-Body Localization in a Controlled Open Quantum System, *Phys. Rev. X* **7**, 011034 (2017).
- [78] Y. S. Patil, S. Chakram, and M. Vengalattore, Measurement-induced localization of an ultracold lattice gas, *Phys. Rev. Lett.* **115**, 140402 (2015).
- [79] N. Dogra, M. Landini, K. Kroeger, L. Hruby, T. Donner, T. Esslinger, Dissipation-induced structural instability and chiral dynamics in a quantum gas, *Science* **366**, 1496 (2019).
- [80] N. Syassen, D. M. Bauer, M. Lettner, T. Volz, D. Dietze, J. J. García-Ripoll, J. I. Cirac, G. Rempe, S. Dürr, Strong dissipation inhibits losses and induces correlations in cold molecular gases, *Science* **320**, 1329 (2008).
- [81] B. Yan, S. A. Moses, B. Gadway, J. P. Covey, K. R. A. Hazzard, A. M. Rey, D. S. Jin, J. Ye, Observation of dipolar spin-exchange interactions with lattice-confined polar molecules, *Nature* **501**, 521 (2013).
- [82] B. Zhu, B. Gadway, M. Foss-Feig, J. Schachenmayer, M. L. Wall, K. R. A. Hazzard, B. Yan, S. A. Moses, J. P. Covey, D. S. Jin, J. Ye, M. Holland, and A. M. Rey, Suppressing the loss of ultracold molecules via the continuous quantum Zeno effect, *Phys. Rev. Lett.* **112**, 070404 (2014).
- [83] T. Tomita, S. Nakajima, I. Danshita, Y. Takasu, Y. Takahashi, Observation of the Mott insulator to superfluid crossover of a driven-dissipative Bose-Hubbard system, *Sci. Adv.* **3**, e1701513 (2017).
- [84] K. Sponselee, L. Freystatzky, B. Abeln, M. Diem, B. Hundt, A. Kochanek, T. Ponath, B. Santra, L. Mathey, K. Sengstock, and C. Becker, Dynamics of ultracold quantum gases in the dissipative Fermi Hubbard model, *Quantum Sci. Technol.* **4**, 014002 (2019).
- [85] M. J. Rice and E. J. Mele, Elementary excitations of a linearly conjugated diatomic polymer, *Phys. Rev. Lett.* **49**, 1455 (1982).
- [86] F. Song, S. Yao, and Z. Wang, Non-Hermitian Skin Effect and Chiral Damping in Open Quantum Systems, *Phys. Rev. Lett.* **123**, 170401 (2019).
- [87] F. Dangel, M. Wagner, H. Cartarius, J. Main, and G. Wunner, Topological invariants in dissipative extensions of the Su-Schrieffer-Heeger model, *Phys. Rev. A* **98**, 013628 (2018).
- [88] Q. B. Zeng, Y. B. Yang, and Y. Xu, Topological phases in non-Hermitian Aubry-André-Harper models, *Phys. Rev. B* **101**, 020201 (2020).
- [89] H. Jiang, L. Lang, C. Yang, S. Zhu, and S. Chen, Interplay of non-Hermitian skin effects and Anderson localization in nonreciprocal quasiperiodic lattices, *Phys. Rev. B* **100**, 054301 (2019).
- [90] S. Longhi, Topological phase transition in non-Hermitian quasicrystals, *Phys. Rev. Lett.* **122**, 237601 (2019).
- [91] D.-W. Zhang, Y.-L. Chen, G.-Q. Zhang, L.-J. Lang, Z. Li, and S.-L. Zhu, Skin superfluid, topological Mott insulators, and asymmetric dynamics in interacting non-Hermitian Aubry-André-Harper models, *arXiv:2001.07088* (2020).
- [92] T. Liu, J. J. He, T. Yoshida, Z.-L. Xiang, and F. Nori, Non-Hermitian topological Mott insulators in 1D fermionic superlattices, *arXiv:2001.09475* (2020).